Highly Active Photocatalytic TiO2 Powders Obtained by Thermohydrolysis of TiCl4 in Water

ARTICLE *in* THE JOURNAL OF PHYSICAL CHEMISTRY C · AUGUST 2009

Impact Factor: 4.77 · DOI: 10.1021/jp904673e

Highly Active Photocatalytic TiO_2 Powders Obtained by Thermohydrolysis of $TiCl_4$ in Water

Agatino Di Paola,*,† Marianna Bellardita,† Riccardo Ceccato,‡ Leonardo Palmisano,† and Francesco Parrino†

"Schiavello-Grillone" Photocatalysis Group, Dipartimento di Ingegneria Chimica dei Processi e dei Materiali, Università di Palermo, Viale delle Scienze, 90128 Palermo, Italy, and Dipartimento di Ingegneria dei Materiali e delle Tecnologie Industriali, Via Mesiano 77, 38050 Trento, Italy

Received: May 19, 2009; Revised Manuscript Received: July 7, 2009

Highly active photocatalytic TiO_2 samples were synthesized by thermohydrolysis of $TiCl_4$ in water at 100 °C. Rutile, binary mixtures of anatase and rutile or anatase and brookite or ternary mixtures of anatase, brookite, and rutile were obtained depending on the $TiCl_4/H_2O$ ratio. Rietveld refinements were employed to evaluate the crystalline phases and composition of the mixtures. The effect of the aging time on the phase composition was also studied. The band gap values of the samples were obtained by the diffuse reflectance spectra. The position of the flat band potentials of anatase, brookite, and rutile was determined measuring the photovoltage as a function of the suspension pH. From these data, the relative positions of the energy bands of the three semiconductors were estimated. 4-Nitrophenol photodegradation was used to evaluate the photoactivity of the various samples. Some powders were more active than Degussa P25. The most efficient samples consisted of a ternary mixture of anatase, brookite, and rutile. The high photocatalytic activity was explained by the presence of junctions among different polymorphic TiO_2 phases that enhance the separation of the photogenerated electron−hole pairs, hindering their recombination.

Introduction

TiO_2 is the most studied photocatalyst for environmental applications because of its high efficiency, nontoxicity, chemical and biological stability, and low cost.[1] TiO_2 exists in three different crystalline habits: anatase, brookite, and rutile. All three crystalline structures consist of deformed TiO_6 octahedra connected differently by corners and edges.[2] Anatase and rutile are the forms more frequently studied because pure brookite is rather difficult to be prepared.

Anatase is generally accepted to be a photocatalyst more efficient than rutile and brookite, but mixtures of the TiO_2 polimorphic phases often show photocatalytic activities superior to those of the pure phases. The enhanced photoactivity has been attributed to a retarded electron/hole recombination due to the junction between different polymorphs.

Degussa P25, that is frequently used as a benchmark in heterogeneous photocatalysis, consists of a mixture of anatase and rutile phases. The first extensive work that correlates the photocatalytic activity and structure of P25 was carried out by Bickley et al.[3] The existence of an intimate contact between anatase and rutile particles was invoked to account for the high photoactivity of this material. Ohno et al.[4] found that the rutile phase does not exist as an overlayer on the surface of the anatase particles[3] but it exists separately from anatase particles.

Kawahara et al. prepared patterned anatase/rutile films and demonstrated that coupling anatase and rutile in a bilayer form increases the photocatalytic activity with respect to the individual components.[5] Zhang et al. prepared mixtures of anatase and rutile that exhibited higher photoactivity than pure anatase or rutile.[6] The activity of anatase−rutile mixtures for the photodegradation of *p*-coumaric acid was comparable or higher than that of Degussa P25.[7] Anatase−rutile coupled particles prepared by a dissolution−reprecipitation method were more active than P25.[8] Nanocrystalline powders with different anatase/rutile ratios were synthesized at low temperature by a microemulsion-mediated hydrothermal method[9] or by a solvothermal process.[10] Jiang et al. prepared nanoporous film electrodes with mixed anatase−rutile phases.[11]

Anatase−brookite composite nanocrystals synthesized by a sonochemical sol−gel method showed a photocatalytic activity higher than that of anatase[12] and P25.[13] The high activity of anatase−brookite mixed samples obtained at low temperature was attributed to the junction between anatase and brookite crystals.[14] Mixed phase samples, both an anatase−brookite composite and the anatase−rutile commercial P25, showed the best performance for the assisted photoreduction of Cr(VI)[15] and the photodegradation of aqueous methyl orange.[16] The photoactivity of anatase−brookite composite nanocrystals was higher than that of a single-phase anatase with a much larger surface area.[17] Mesoporous mixed brookite−anatase films were prepared by dip coating and tested as electrodes for dye-sensitized solar cells.[18]

Mixtures of brookite and rutile were obtained by thermolysis of $TiCl_4$ in diluted HCl solutions.[19−22] The photoactivity of the mixed powders was higher than that of rutile but comparable with that of brookite.[22] Recently, Wei et al. prepared mixed brookite and rutile nanoparticles from aqueous $TiCl_3$ solutions, using methylcellulose and NaCl as additives.[23]

Ternary (anatase, brookite, and rutile) mixtures synthesized by the hydrolysis of titanium tetrabutoxide in ethanol, HCl, and water decomposed 2,2-dinitroaniline more efficiently than binary (anatase and brookite) mixtures or P25.[24] The photocatalytic activity of tricrystalline powders obtained by thermohydrolysis of $TiCl_4$ in NaCl aqueous solutions was fairly good and superior

* Corresponding author. E-mail: dipaola@dicpm.unipa.it.
† Università di Palermo.
‡ Dipartimento di Ingegneria dei Materiali e delle Tecnologie Industriali.

10.1021/jp904673e CCC: $40.75
Published on Web 07/30/2009

to that of brookite or rutile.[22] Triphasic titania microspheres with high photocatalytic activity were synthesized using $TiCl_4$ and $FeCl_3$ in the presence of a nonionic surfactant.[25]

The sol−gel technique has been usually employed to produce TiO_2 catalysts. Further hydrothermal treatments allow the production of nanocrystallites having a wide range of composition. The phase selection depends on the reactant concentration, temperature, and reaction time. The syntheses are generally followed by calcination of the resulting materials.

Titanium(IV)alkoxides have been frequently studied as titanium precursors, but their high cost and the need to handle organic solvents are important drawbacks. Inorganic precursors are preferable, and TiO_2 powders have been often prepared by hydrolysis of $TiCl_4$, generally in aqueous acidic solutions.[22,26,27] Only few works have concerned the hydrolysis of $TiCl_4$ in pure water.[28,29]

In this study, we report the synthesis of highly active TiO_2 photocatalysts obtained under mild experimental conditions by thermohydrolysis of $TiCl_4$ in pure water at 100 °C. The preparation method is very simple and does not require the use of expensive thermal or hydrothermal treatments. Depending on the $TiCl_4/H_2O$ ratio, pure rutile, binary mixtures of anatase and rutile or anatase and brookite, or ternary mixtures of anatase, brookite, and rutile can be obtained. The reactivity of all samples was tested for the photocatalytic degradation of 4-nitrophenol and compared to that of commercial rutile (Tioxide) and Degussa P25 TiO_2 samples.

Experimental Section

Sample Preparation. Titanium tetrachloride (Fluka 98%) was used as a starting material without any further purification. A 1 mL portion of $TiCl_4$ was slowly added to different volumes of distilled water at room temperature. The hydrolysis reaction was highly exothermic and produced high quantities of fumes of HCl. After continuous stirring, clear transparent solutions were obtained when the $TiCl_4$ concentration was high. In the presence of $TiCl_4/H_2O$ ratios lower than 1:10, only permanent dispersions were obtained so that the least concentrated samples were prepared by diluting with water the 1:5 solution until the desired $TiCl_4/H_2O$ ratio was reached.

The solutions were heated in closed bottles and aged at 100 °C in an oven for 48 h. The bottles were allowed to cool to room temperature, and the resultant solids were recovered using a vacuum pump at 55 °C. The samples were identified according to the notation $TiO_2(1{:}x)$ where $1{:}x$ represents the $TiCl_4/H_2O$ ratio.

Some samples were dialyzed (Dialysis Tubing Cellulose Membrane with MW 12 400 cut off pores) or calcined for 2 h at different temperatures.

Anatase, brookite, and rutile samples were also prepared to obtain information on the position of the band energy levels of these pure phases. Brookite was separated by peptization from a binary mixture of brookite and rutile, obtained by thermolysis of a solution of $TiCl_4$ in diluted HCl ($TiCl_4$:H_2O:HCl volume ratio 1:300:20) at 100 °C for 48 h.[22] After repeated washings with water, a dispersion of brookite particles formed while the rutile phase remained as precipitate. The sol containing the brookite particles and the precipitate of rutile were separately dried under vacuum at 55 °C. Anatase was prepared by boiling an aqueous solution of $TiCl_4$ ($TiCl_4$:H_2O volume ratio 1:50) for 2 h.[30] After removal of the supernatant liquid, the solid was dried under vacuum at 55 °C.

Sample Characterization. X-ray diffraction spectra of the powders were recorded at room temperature using a powder diffractometer (Rigaku D-max) employing the Cu Kα radiation and a graphite monochromator in the diffracted beam. Typical scans were performed in the 2θ 10−110° range, with a sampling range of 0.05° and 5 s counting time; both 0.5° divergence and antiscattering slits were used. Experimental spectra were compared for the qualitative analyses with the corresponding powder diffraction file (PDF) cards for the three titanium dioxide polymorphs: anatase (21-1272), rutile (21-1276), and brookite (29-1360). Quantitative analyses of the samples were performed using a modified Rietveld method,[22,31] developed for the determination of amorphous and crystalline phases in ceramic materials, under the assumptions of the model developed by Le Bail.[32] Moreover, the method allows the evaluation of the crystallite dimensions from the line profile analysis based on the Warren−Averbach theory.[33]

Nitrogen physisorption experiments were performed at the liquid nitrogen temperature using a Micromeritics ASAP 2010 system. All the samples were degassed below 1.3 Pa at 25 °C prior to the measurement. The specific surface area (SSA) values were calculated by the BET equation in the interval $0.05 \leq (p/p_o) \leq 0.33$. Pore size distribution was calculated using the BJH method applied both on the adsorption and the desorption branches of the isotherms.

Transmission electron microscopy (TEM) observations were performed using a transmission electron microscopy (JEOL JEM-2000 FX) operating at 200 kV. The samples were prepared by sonicating a diluted suspension of powder in water (ca. 10 mg in 1 L of H_2O) for 10 min and depositing a drop of this suspension on a Cu grid support.

Ultraviolet−visible spectra were obtained by diffuse reflectance spectroscopy using a Shimadzu UV-2401 PC instrument. $BaSO_4$ was used as a reference, and the spectra were recorded in the range 200−800 nm.

The values of the flat-band potentials of anatase, brookite, and rutile were determined by the slurry method proposed by Roy et al.[34] Two different electron acceptors were used: MV^{2+} (methyl viologen dichloride; 1,1′-dimethyl-4,4′-bipyridinium dichloride; $E_{MV}{}^{2+/+\cdot} = -0.45$ V vs NHE)[35] for anatase or brookite, and DP^{2+} (4,5-dihydro-3a,5a-diaza-pyrene-dibromide; $E_{DP}{}^{2+/+\cdot} = -0.27$ V vs NHE for rutile).[36,37] A 30 mg portion of catalyst and 6 mg of electron acceptor were suspended in 50 mL of a 0.1 M KNO_3 solution. A platinum electrode and Ag/AgCl served as working and reference electrodes, respectively. The suspensions were magnetically stirred and purged with nitrogen throughout the experiment. The pH was adjusted with 0.1 M HNO_3 or 0.1 M NaOH solutions. The light source was an Osram XBO 150 W xenon arc lamp. The photovoltage developed was recorded and plotted versus pH.

Photoreactivity Experiments. A Pyrex batch photoreactor of cylindrical shape containing 0.5 L of aqueous suspension was used. A 125 W medium pressure Hg lamp (Helios Italquartz, Italy) was immersed within the photoreactor and the photon flux emitted by the lamp was $\Phi_i = 13.5$ mW cm^{-2}; it was measured by using a radiometer "UVX Digital" leaned against the external wall of the photoreactor containing only pure water. O_2 was continuously bubbled for ca. 0.5 h before switching on the lamp and throughout the occurrence of the photoreactivity experiments. The temperature inside the reactor was ca. 30 °C.

The amount of catalyst was 0.6 g L^{-1} and the initial 4-nitrophenol (BDH) concentration was 20 mg L^{-1}. Samples of 5 mL were withdrawn at fixed intervals of time with a syringe, and the catalyst was separated from the solution by filtration through 0.1 μm Teflon membranes (Whatman). Some

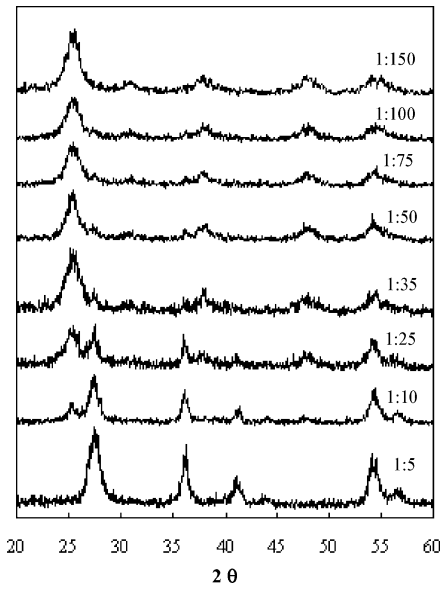

Figure 1. XRD patterns of the solids obtained by thermohydrolysis of $TiCl_4$ in water at 100 °C for 48 h. 1:*x* represents the $TiCl_4/H_2O$ (v/v) ratio.

drops of a 1 M NaOH solution were added before filtration to cause agglomeration of the particles. The quantitative determination of 4-nitrophenol was performed by measuring its absorption at 315 nm with a spectrophotometer Shimadzu UV-2401 PC.

Results

X-ray Diffraction. Binary or ternary mixtures of the three polimorphs of TiO_2 were prevalently obtained by thermohydrolysis of $TiCl_4$ in water at 100 °C. The composition of the powders depended on the $TiCl_4/H_2O$ ratio and on the aging time. Figure 1 shows the XRD patterns of the solids formed after 48 h of heating. The percentages of anatase, brookite, and rutile present in the various samples are reported in Table 1.

When $TiCl_4$ hydrolyses, it generates TiO_2 as well as H^+ and Cl^- ions. The H_2O content is the major factor in determining the crystalline phases and their relative proportions. Figure 2 shows the influence of the $TiCl_4/H_2O$ ratio on the percentages of the three phases. Anatase increased with a decreasing $TiCl_4/H_2O$ ratio, whereas brookite appeared for $[TiCl_4] < 0.34$ M. The percentages of anatase and brookite were scarcely influenced when the $TiCl_4/H_2O$ ratio was lower than 1:50. The fraction of rutile decreased with dilution and, this is consistent with the results of previous works indicating that low pH values favor the formation of rutile.[19−22] Only rutile was obtained when the $TiCl_4/H_2O$ ratio was 1:5.

The relative proportions of anatase, brookite, and rutile also depended on the duration of aging. Table 2 reports the composition of the mixtures obtained by thermolysis of three $TiCl_4$ solutions for different reaction times. Anatase and rutile increased by aging the samples from 24 to 48 h, but their percentages decreased after 76 h. Conversely, brookite initially decreased and then increased.

Tables 1−3 report the crystallite dimensions of the TiO_2 powders prepared under different experimental conditions. All the samples were nanocrystalline, and the mean diameter of the crystallites ranged between 2.2 and 12.6 nm. In each mixture, the size of the rutile crystallites was always higher than that of anatase and brookite. Rutile size increased with a decreasing $TiCl_4/H_2O$ ratio while the mean size of anatase and brookite crystallites was practically independent of $TiCl_4$ concentration. As shown in Table 2, only the crystallite size of rutile substantially increased with increasing the aging time.

TABLE 1: Effect of the $TiCl_4/H_2O$ Ratio on the Relative Content (wt %) and Crystallite Size (ϕ) of Anatase, Brookite, and Rutile, Specific Surface Area (SSA), and Initial Reaction Rate (r_0)[a]

sample	$[TiCl_4]$ [mol L^{-1}]	wt %	ϕ [nm]	SSA [m^2 g^{-1}]	$r_0 \times 10^9$ [mol L^{-1} s^{-1}]
TiO_2(1:5)	1.48	A −	A −	87.5	31
		B −	B −		
		R 100	R 3.5		
TiO_2(1:10)	0.81	A 19	A 3.8	108.0	63
		B −	B −		
		R 81	R 4.3		
TiO_2(1:25)	0.34	A 53	A 2.2	201.5	61
		B −	B −		
		R 47	R 4.4		
TiO_2(1:35)	0.25	A 70	A 2.2	196.1	47
		B 19	B 2.6		
		R 11	R 6.0		
TiO_2(1:50)	0.17	A 66	A 2.9	196.6	58
		B 21	B 3.4		
		R 13	R 6.2		
TiO_2(1:75)	0.12	A 65	A 2.4	216.1	76
		B 28	B 2.5		
		R 7	R 9.0		
TiO_2(1:100)	0.09	A 66	A 2.3	219.1	67
		B 28	B 3.1		
		R 6	R 6.0		
TiO_2(1:150)	0.06	A 77	A 2.1	208.3	33
		B 23	B 3.0		
		R −	R −		

[a] The samples were obtained after 48 h of aging at 100 °C.

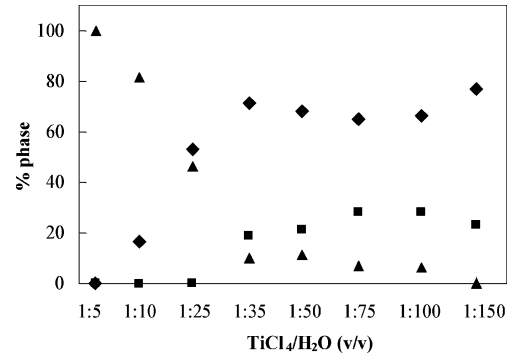

Figure 2. Influence of the $TiCl_4/H_2O$ ratio on the relative percentages of (♦) anatase, (■) brookite, and (▲) rutile. The solids were obtained by thermohydrolysis of $TiCl_4$ in water at 100 °C for 48 h.

Different aliquots of the TiO_2(1:50) sample were heated in an oven for 2 h at 300 and 450 °C. Table 3 shows the effect of the temperature on the phase composition of the products. At 300 °C, both anatase and rutile increased while brookite decreased. At 450 °C, anatase decreased and rutile increased. The crystallite size of the three polymorphs increased with increasing temperature. In particular, heating the powders at 450 °C increased the anatase and rutile sizes by approximately 80% and 88%, respectively. The increase of brookite size was higher, about 185%.

Specific Surface Areas. Data evaluated from the physisorption measurements are reported in Tables 1−3. The specific surface areas of the binary and ternary mixtures were somewhat high and not very dependent on the $TiCl_4/H_2O$ ratio. The TiO_2(1:5) sample consisting of only rutile revealed an SSA value (88 m^2 g^{-1}) noticeably greater than that of commercial rutile Tioxide (8 m^2 g^{-1}). A reduction of SSA was observed as a consequence of the thermal treatment at 300 and 450 °C.

TABLE 2: Effect of the Aging Time on the Relative Content (wt %) and Crystallite Size (ϕ) of Anatase, Brookite, and Rutile, Specific Surface Area (SSA), and Initial Reaction Rate (r_0)

sample	time [h]	wt %	ϕ [nm]	SSA [m^2 g^{-1}]	$r_0 \times 10^9$ [mol L^{-1} s^{-1}]
TiO_2(1:25)	24	A 72	A 2.0	230.0	44
		B 23	B 2.7		
		R 5	R 4.1		
TiO_2(1:25)	48	A 53	A 2.2	201.5	61
		B −	B −		
		R 47	R 4.4		
TiO_2(1:25)	76	A 45	A 2.3	193.3	49
		B 13	B 2.8		
		R 41	R 4.7		
TiO_2(1:50)	24	A 57	A 1.9	224.7	57
		B 37	B 3.1		
		R 6	R 4.0		
TiO_2(1:50)	48	A 67	A 2.9	196.6	58
		B 20	B 3.4		
		R 13	R 6.2		
TiO_2(1:50)	76	A 55	A 2.2	191.6	45
		B 42	B 3.2		
		R 3	R 7.0		
TiO_2(1:75)	24	A 59	A 1.8	204.9	48
		B 38	B 2.6		
		R 3	R 5.0		
TiO_2(1:75)	48	A 65	A 2.4	216.1	76
		B 28	B 2.5		
		R 7	R 9.0		
TiO_2(1:75)	76	A 56	A 2.3	190.1	40
		B 42	B 2.4		
		R 1	R10.0		

TABLE 3: Effect of the Thermal Treatment on the Relative Content (wt %) and Crystallite Size (ϕ) of Anatase, Brookite, and Rutile, Specific Surface Area (SSA), and Initial Reaction Rate (r_0) of the TiO_2(1:50) Sample Calcined for 2 h at Different Temperatures

sample	wt %	ϕ [nm]	SSA [m^2 g^{-1}]	$r_0 \times 10^9$ [mol L^{-1} s^{-1}]
TiO_2(1:50)	A 67	A 2.9	196.6	58
	B 20	B 3.4		
	R 13	R 6.2		
TiO_2(1:50, 300 °C)	A 74	A 3.2	114.0	15
	B 14	B 4.0		
	R 12	R 8.9		
TiO_2(1:50, 450 °C)	A 66	A 4.3	72.0	16
	B 14	B 5.7		
	R 20	R 12.6		

Figure 3 shows representative examples of the nitrogen adsorption−desorption isotherms obtained with the various powders. All samples displayed hysteresis loops in their isothermal curves, as evidence of the presence of mesoporosity from the desorption branch. According to the IUPAC classification,[38] type IIb isotherms (Figure 3a) and hysteresis loops of type H3 were detected for the samples TiO_2(1:5) and TiO_2-(1:10) containing only rutile or a high content of rutile (81%), respectively. Differently, type IVb isotherms (Figure 3b) and hysteresis loops of type H2 were displayed by the samples consisting of binary and ternary mixtures of the TiO_2 polymorphs. The thermal treatment led to a progressive vanishing of the plateau region at higher relative pressure values with a corresponding decrease of the surface area. A type IIb isotherm (Figure 3c), but with a hysteresis loop of type H3, was obtained for the sample TiO_2(1:50) calcined at 450 °C.

The mean pore size diameter of the various samples (around 4 nm) was not influenced by the $TiCl_4/H_2O$ ratio. The thermal

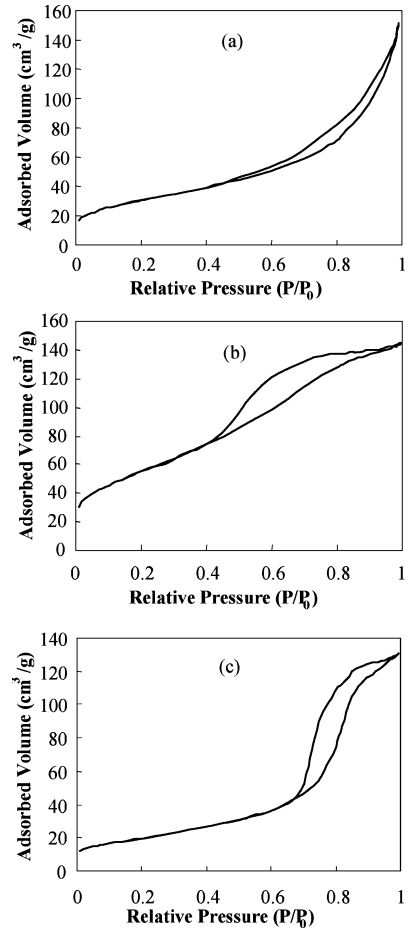

Figure 3. N_2 adsorption−desorption isotherms: (a) TiO_2(1:10); (b) TiO_2(1:25); (c) TiO_2(1:50) calcined at 450 °C.

treatments caused an increase of the pore size: from the desorption branch, the maximum of the distribution curve shifted from 4 nm up to 8 nm when the TiO_2(1:50) sample was calcined at 450 °C.

TEM Analysis. TEM observations revealed that all the samples consisted of aggregates of particles whose sizes appeared generally bigger (30−60 nm) than those calculated from the XRD patterns. Figure 4 shows representative TEM micrographs of the sample TiO_2(1:50). Distinguishing among anatase, brookite, or rutile is challenging because the various particles showed no qualitative differences of shape or morphology. The small crystallites of different phases are probably interwoven with each other forming tightly bound nanoclusters. As shown in Figure 4b, the effect of dialysis was to reduce the size of the aggregates.

Diffuse Reflectance Spectroscopy. Figure 5 shows the diffuse reflectance spectra of pure anatase, brookite, and rutile. TiO_2 is an indirect semiconductor[39] so that the band gap energy, E_g, of the samples can be determined from the tangent lines to the plots of the modified Kubelka−Munk function, $[F(R'_\infty)h\nu]^{1/2}$, versus the energy of the exciting light.[40] As shown in the inset of Figure 5, the E_g values of anatase, brookite, and rutile were 3.05, 3.26, and 2.95 eV, respectively.

The band gap values of the samples obtained by thermohydrolysis of $TiCl_4$ in H_2O at 100 °C ranged between 2.97 and 3.02 eV and were scarcely dependent on the $TiCl_4/H_2O$ ratio and aging time.

Photoelectrochemical Measurements. The position of the flat band potential (E_{FB}) of the three pure TiO_2 polymorphic phases was determined measuring the photovoltage as a

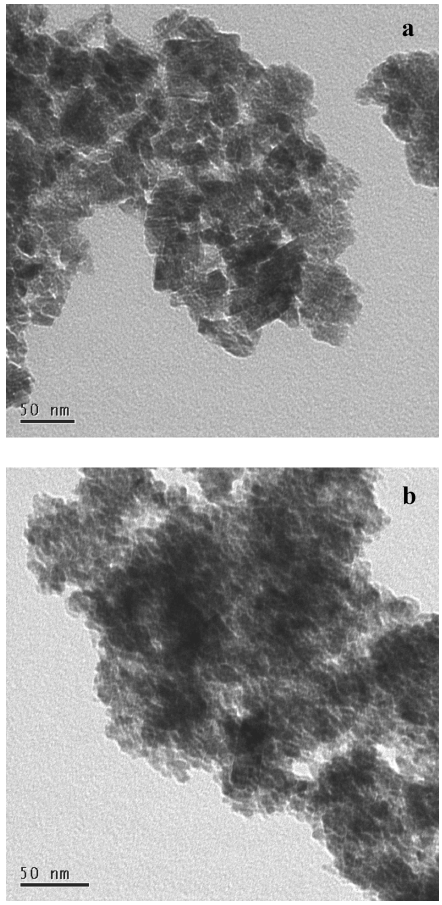

Figure 4. TEM images of the sample TiO_2(1:50) obtained by thermohydrolysis of $TiCl_4$ in water at 100 °C for 48 h: (a) as prepared; (b) after dialysis.

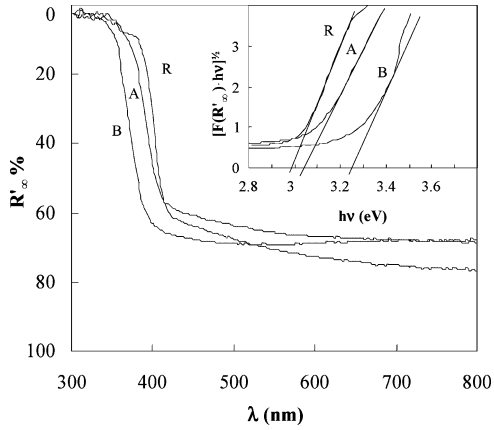

Figure 5. Diffuse reflectance spectra of the home prepared pure TiO_2 samples: (A) anatase, (B) brookite, and (R) rutile. (inset) Plots of the square root of the modified Kubelka−Munk function vs the energy of the absorbed light.

function of the suspension pH in the presence of an electron acceptor.[34] Figure 6 shows the effect of pH on the photovoltage developed on irradiation of anatase, brookite, and rutile suspensions. The pH value of the inflection point (pH_0) allows to calculate the flat band potential at pH 7 by the equations: E_{FB} (pH = 7) = $E_{MV}{}^{2+/+\cdot}$ + 0.059 (pH_0 −7) for anatase and brookite or E_{FB} (pH = 7) = $E_{DP}{}^{2+/+\cdot}$ + 0.059 (pH_0 −7) for rutile. The values obtained were − 0.45 V for anatase, − 0.46 V for brookite, and − 0.37 V for rutile.

Photoreactivity experiments. The disappearance of 4-nitrophenol was followed by determining the concentration of the

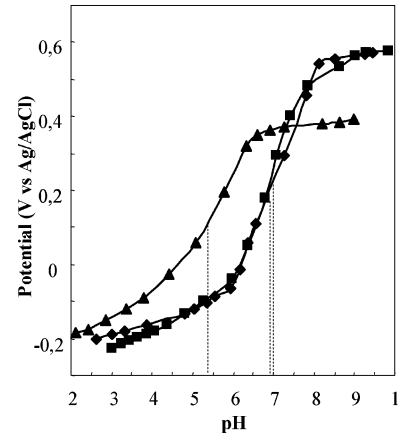

Figure 6. Effect of pH on the photovoltage developed on irradiation of (♦) anatase, (■) brookite, and (▲) rutile suspensions.

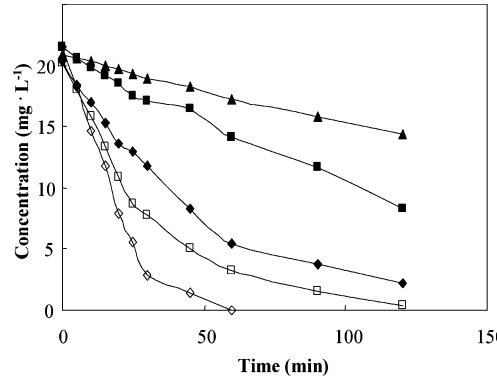

Figure 7. 4-Nitrophenol photodegradation curves of various samples: (♦) anatase, (■) brookite, (▲) rutile, (◇) TiO_2 (1:75), (□) Degussa P25.

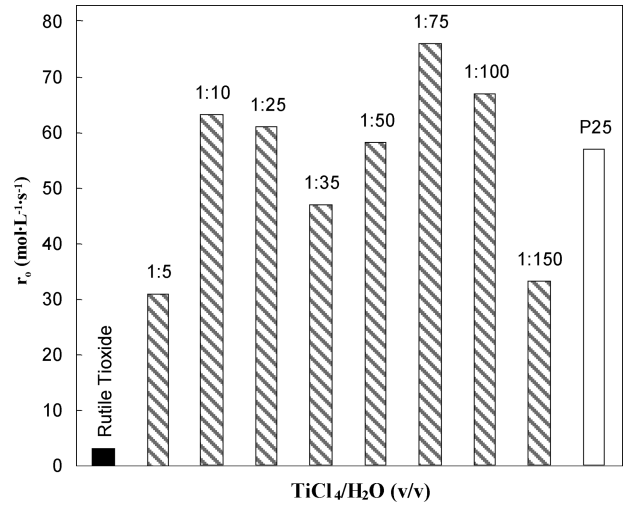

Figure 8. Initial reaction rates for the photodegradation of 4-nitrophenol.

substrate at various time intervals. Figure 7 shows the results obtained in the presence of some representative samples. Commercial TiO_2 Degussa P25 was also tested for comparison. The degradation rate, r_0, was calculated from the initial slope of the concentration versus time profiles. The various values of r_0 are reported in Tables 1−3.

As shown in Figure 8, the photocatalytic activity of the powders obtained by thermolysis of $TiCl_4$ depended on the $TiCl_4/H_2O$ volume ratio. The various samples revealed performances similar or better than that of Degussa P25 (r_0 = 57 mol

L^{-1} s^{-1}) with the exception of TiO_2(1:150) and TiO_2(1:5). The most active powders were ternary mixtures of anatase, brookite and rutile whereas TiO_2(1:150) contained a binary mixture of anatase and brookite, and TiO_2(1:5) consisted of only rutile. It is worth noting that, differently from a commercial rutile Tioxide sample which was practically inactive, the r_0 value determined for TiO_2(1:5) was more than half of that of Degussa P25. The sample showing the highest photoactivity was TiO_2(1:75).

Total organic carbon (TOC) measurements revealed that 4-nitrophenol was completely mineralized in the presence of the samples obtained by thermohydrolysis of $TiCl_4$ in water, and the rate of mineralization of the most active samples was higher than that of P25.

To verify if the high efficiency of the mixed samples was due to the simple coupling of different semiconductors, the photodegradation of 4-nitrophenol was studied in the presence of a mechanical mixture of anatase, brookite, and rutile. Although the composition of the physical mixture was the same of that of TiO_2(1:75), the initial reaction rate was only 25×10^{-9} mol L^{-1} s^{-1}, i.e. one-third of the value determined for the corresponding powder obtained by thermohydrolysis.

The r_0 values reported in Table 2 show that the photoactivity of the various samples increased with increasing aging times, reached a maximum value and afterward decreased. The r_0 values progressively decreased if the solids obtained at 100 °C were subsequently calcined at 300 or 450 °C (see Table 3). Similarly, the sample TiO_2(1:50) subjected to dialysis was less active than the initial suspension (r_0 decreased from 58 to 31 $\times 10^{-9}$ mol L^{-1} s^{-1}).

Discussion

Nanostructured TiO_2 powders can be prepared by thermohydrolysis of $TiCl_4$ in water at 100 °C. According to Zheng et al., a low concentration $TiCl_4$ solution contains a large amount of $[Ti(OH)_2(OH_2)_4]^{2+}$ octahedral complexes.[28] As a consequence of hydrothermic treatments, the octahedra link together by olation, through dehydration reactions between aquo and hydroxo ligands. Rutile-type nuclei are developed if the $[Ti(OH)_2(OH_2)_4]^{2+}$ monomers combine by sharing equatorial edges, whereas anatase- or brookite-type nuclei form if the monomers combine by sharing apical edges.[28] Further growth proceeds by formation of linear chains from the rutile-type nuclei or of skewed chains from the anatase- or brookite-type nuclei. All the three polymorphic phases can be obtained contemporaneously, and the composition of the mixtures depends on the $TiCl_4/H_2O$ ratio and by the reaction time.

When the concentration of $TiCl_4$ is high, the solution should prevalently contain $[TiO(OH_2)_5]^{2+}$ momomers that can combine by olation only by sharing equatorial edges. In this case, rutile crystallites are developed.[28]

Our experimental results have shown that the relative proportions of the TiO_2 polymorphic phases depend on the initial concentration of $TiCl_4$, i.e. the $TiCl_4/H_2O$ ratio. Anatase, rutile, and a significant amount of brookite were always found when $[TiCl_4] < 0.25$ M, whereas a mixture of anatase and rutile or only rutile were obtained for higher values of concentration. Rutile was absent when $[TiCl_4] = 0.06$ M.

The presence of rutile in the more concentrated samples is in agreement with the results of Cheng et al. reporting that high acidity and high Cl^- concentrations are beneficial to the formation of the rutile phase.[41] The $TiCl_4/H_2O$ ratio plays an important role in the competition between the formation of anatase and rutile but has little effect on brookite formation. The fraction of rutile became lesser with increasing reaction time although its crystalline size continued to grow probably via a dissolution and precipitation process (Ostwald ripening).[42] Aging duration did not significantly influence the crystallite size of anatase and brookite.

The results of the thermohydrolytic treatment at 100 °C were somewhat different from those obtained by simple boiling of the $TiCl_4$ solutions.[30] In the latter case, only the anatase phase was practically obtained although small amounts of rutile were found when the $TiCl_4$ concentration was high. The reason is probably the continuous evaporation of HCl that caused an increase of the solution pH favoring the formation of anatase.

A mixture of rutile as the major product and anatase as the minor product was obtained by Zheng et al. when the hydrothermal process was carried out at 200 °C for 24 h.[28] A small amount of brookite was only found when $[TiCl_4]$ was 1 M. The composition of the various mixtures was related to the synthesis conditions and the fraction of rutile increased with increasing temperature. These results are not at variance with the findings obtained by heating the representative TiO_2(1:50) sample at 300 and 450 °C since the increase of reaction temperature accelerates the phase transformation from thermodynamic metastable phases as anatase and brookite to the stable rutile phase. The identical values of brookite percentages found at 300 and 450 °C suggest that the decrease of anatase and the corresponding increase of rutile are due to the transformation from anatase into rutile. The apparent increase of anatase at the expense of brookite observed by heating the sample at a relatively low temperature as 300 °C is probably caused by the crystallization of the unknown amorphous content of the powder.

All the samples prepared by thermohydrolysis of $TiCl_4$ at 100 °C had high specific surface areas and small particle sizes. The diameter of the crystallites determined by the TEM micrographs revealed that all the samples were nanostructured. By thermal treatment, the surface area decreased indicating the growth of particles larger than those of the starting power.

The samples TiO_2(1:5) and TiO_2(1:10) containing only rutile or a high content of rutile showed typical type II isotherms. This indicates the existence of a nonporous matrix in agreement with data reported for titanium dioxide powders.[43] Differently, the type IVb isotherms displayed by the samples containing binary and ternary mixtures, associated with the presence of a H2-type hysteresis loops, reveal a complex interconnected network of micro- and mesopores with different dimensions and shapes, which is typical of several oxide gels.[38]

The diffuse reflectance measurements have allowed the determination of the band gap of the various samples. The values of 3.26 and 2.98 eV estimated for brookite and rutile are in good agreement with those found in literature, 3.26[44] and 3.0 eV,[1] respectively. The band gap of 3.05 eV determined for anatase is lower than that usually reported (3.20 eV[1]), but it should be recalled that our sample, obtained at low temperature, is not well crystallized.[30] The band gaps of the mixtures of two or three phases were lower than those of anatase and brookite and near to that of rutile. In accord with the results by Torimoto et al.,[45] the E_g values of the mixed TiO_2 powders were practically independent of anatase and brookite, reflecting the presence of the rutile phase having a lower energy gap.

The value of -0.45 V estimated for the flat band potential of anatase at pH = 7 is in excellent agreement with the -0.46 V found by Ward et al. from photocurrent measurements,[46] but it is less negative than the -0.57 V determined for an anatase single crystal by means of Mott−Schottky plots.[47] The potential value of -0.37 V measured for rutile does not differ significantly from the -0.34 V reported by Kalyanansundaram and Grätzel,[48]

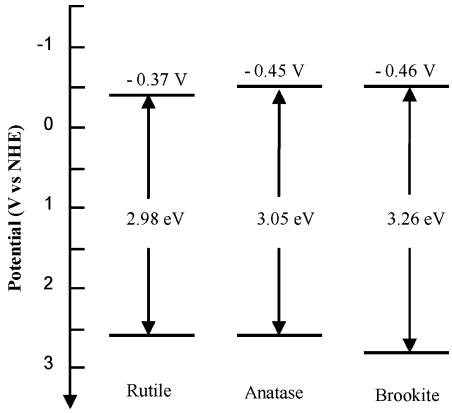

Figure 9. Electrochemical potentials (versus NHE) of the band edges of anatase, brookite, and rutile at pH = 7.

but according to Kavan et al., the flat-band potential of rutile should be shifted positively by 0.2 V with respect to the flat-band potential of anatase.[47] Radecka et al. compared the values of E_{FB} for different forms of anatase and rutile and at pH = 7 the values ranged between −0.42 and −0.57 V for anatase and between −0.33 and −0.44 V for rutile.[49] The difference between these values might be attributed to differences in the nature of the material (powder, single crystal, film) or to the different methods of estimating E_{FB}.

To the best of our knowledge, no determinations of the flat-band potential of brookite are reported in literature. Grätzel and Rotzinger estimated the E_{FB} value of brookite as −0.44 V by extended Hückel molecular orbital (MO) calculations.[50] This theoretical value is practically coincident with the −0.46 V determined in this work.

Assuming that the difference between flat band potential and conduction band edge is negligible, it is possible to locate the valence band edge of the three semiconductors by adding the band gap energy to the flat-band potential value. Figure 9 shows the relative positions of the energy bands of anatase, brookite, and rutile, at pH = 7. Anatase and brookite differ in the position of their valence band since brookite has a slightly larger band gap energy.

The high photoactivity exhibited by the mixed powders obtained by thermohydrolysis of $TiCl_4$ in water seems to depend prevalently on the contemporaneous presence of different TiO_2 polimorphic phases. The coupling of semiconductors possessing different redox energies for their corresponding conduction and valence bands allows more efficient charge separation to be achieved and enhances the efficiency of the interfacial charge transfer to adsorbed substrates.[51]

The elevated activity of a rutile−anatase mixture as Degussa P25 has been attributed to the transfer of electrons from the conduction band of anatase to that of rutile.[3,8,11] According to Yan et al. when anatase interweaves with rutile, the electrons from anatase phase transfer to rutile, while the holes transfer from rutile to anatase.[52] Therefore, the anatase−rutile mixed phase hinders the electron−hole recombination by locating electrons and holes in different crystalline phases.

As shown in Figure 9, the conduction band of rutile lies at a potential more positive than the conduction band of anatase while the valence bands are located at the same potential. Under UV irradiation, both semiconductors are simultaneously activated. From the relative position of the band edges, it can be expected that electrons pass from the conduction band of anatase into the conduction band of rutile, but results obtained from the photocatalytic activity of mixed anatase−rutile particles in the photooxidation of naphthalene demonstrated that the electrons are effectively transferred from rutile to anatase.[53] Recently, Hurum et al. proposed that the great photoeffectiveness of Degussa P25 and other mixed anatase−rutile catalysts was due to the stabilization of charge separation by electron transfer from rutile to anatase trapping sites lower in energy than the anatase conduction band.[54] Leytner and Hupp determined that these electron trapping sites lie 0.8 eV below the conduction band of anatase.[55] Electron paramagnetic resonance measurements have probed that in Degussa P25 electron transfer effectively occurs from rutile to anatase and hinders charge recombination.[56] Subsequent electron-transfer moves the electrons from anatase trapping sites to surface trapping sites, further separating the electron−hole pairs. By analogy, the enhanced photoactivity shown by the samples TiO_2(1:10) and TiO_2-(1:25) constituted by anatase−rutile mixtures is attributable to the increased charge separation efficiency due to the vectorial displacement of electrons between anatase and rutile particles. The proximity of anatase to rutile allows to scavenge rutile electrons and stabilize the charge separation, preventing rapid recombination. The contact is very efficient due to the small sizes of the crystallites.

The most active powders obtained by thermolysis of $TiCl_4$ in water consisted of a mixture of anatase, brookite, and rutile. This finding agrees with the results of previous works reporting that ternary mixtures of the TiO_2 polimorphic phases were more efficient of pure anatase, brookite, and rutile or of binary mixtures of the three polimorphs.[22,24] Wei et al. attributed the high photocatalytic activity of titania microspheres to the synergetic effect of Fe-doping and the presence of anatase, brookite, and rutile mixing.[25] The existence of interfaces among different phases probably allows electron transfer from rutile to anatase−brookite hindering charge recombination.

The photocatalytic process depends critically on the interface between the TiO_2 phases and the particle size. The X-ray results revealed that the rutile crystallites obtained by thermohydrolysis of $TiCl_4$ were atypically small, of the same order of magnitude as anatase and brookite. The rutile crystallites are probably interwoven with the anatase or brookite crystallites facilitating the efficient electron transfer at the various interfaces. The reduced size of the particles leads to larger surface areas, and consequently, the number of available surface active sizes increases. The absence of intimate contact among the particles is probably the cause of the low efficiency of the mechanical mixture with the same composition of the active TiO_2(1:75) sample.

The photoactivity of the mixed powders depends on the composition, the aggregates size, and the distribution of the various junctions among different phases. The decreased efficiency exhibited by the dialyzed sample is justified by the reduction of the dimensions of the particles. Dialysis did not affect the content of anatase, brookite, and rutile of the sample but caused an observable increase of the number of particles as tested by the TEM micrographs. Anyway, the beneficial effect of the presence of smaller particles is probably counteracted by the appearance of particles consisting of single phases.

The photoactivity of the sample TiO_2(1:150) containing a mixture of anatase and brookite was about half that of the ternary mixtures of anatase, brookite, and rutile. Contrasting results on the photocatalytic behavior of mixed anatase−brookite samples are cited in the literature. Ozawa et al. found that anatase−brookite composite nanocrystals exhibited a high photocatalytic activity for the gas-phase oxidation of CH_3CHO,[14] and the photoactivity decreased with increasing the brookite content from 34.6 to

44.8%. Yu et al. reported that the photoactivity of powders containing anatase and brookite exceeded that of Degussa P25.[12,13] Anatase−brookite nanocrystalline samples with an anatase/brookite ratio of 70/30 were found to be more active than commercial anatase samples.[17] The high photocatalytic activity of the anatase−brookite mixtures was attributed to an increased charge separation efficiency due to the anatase−brookite coupling as in the anatase−rutile systems.[14]

Li et al. found that a small amount of brookite in anatase is unfavorable to the improvement of its photoactivity,[57] and Ovenstone presented some evidence that samples containing both anatase and brookite were less active than anatase for the photodecomposition of a solution of acetic acid.[58] The photoactivity of anatase and brookite mixed samples with high (36%) and low (12%) brookite content was similar to that of Degussa P25 but decreased with increasing the brookite content.[16]

Ovenstone suggested that brookite inhibits the photocatalytic activity because the interface between anatase and brookite might act as a site for the recombination of electrons and holes.[58] According to Isley et al., brookite may simply not contribute to the photocatalytic activity so that the particles with high brookite content are less active than those with low brookite content.[16]

Interestingly, an appreciable photoactivity was revealed by the TiO_2(1:5) sample consisting of only rutile. Literature reports that rutile is active or inactive according to the preparation conditions.[59] Zhang et al. found that nanosized rutile with a crystallite size of 7.2 nm was more efficient of ultrafine anatase for the photodegradation of phenol.[60] A fair photoactivity, higher than that of commercial rutile Tioxide, was exhibited by nanosized rutile samples obtained by hydrolysis of $TiCl_4$ in HCl solutions,[22,61] and ultrafine rutile with a high specific surface area was much more photoactive than P25 in the removal of metal ions from aqueous metal−EDTA solutions.[62] The low activity of rutile may be due to its reduced surface area rather than to the crystal structure itself. The low crystallite size and the corresponding high surface area can justify the photocatalytic activity of the TiO_2(1:5) sample.

The efficiency of the mixed systems studied in this work strongly depended on the relative amounts of the phases present in the various samples so that an optimum ratio among anatase, brookite, and rutile may exist in TiO_2(1:75). A long aging time (76 h) appears to be a leveling factor because the photoactivity of the various samples was practically identical even if the $[TiCl_4]/[H_2O]$ ratios were very different (see Table 2). Thermal treatments seem unfavorable for improving the photoactivity of the samples (see Table 3).

Conclusions

Highly active TiO_2 photocatalysts can be prepared by simple hydrolysis of $TiCl_4$ in water under very mild experimental conditions. The photocatalytic activity of some samples was higher than that of Degussa P25 for the degradation of 4-nitrophenol. The high efficiency seems to depend on the contemporaneous presence of two or three TiO_2 polimorphic phases. The small size of the particles and the intimate contact with each other that the comparable size allows are crucial factors to increase the photoactivity of the samples.

The technique presented here is an economical and fast way for the preparation of active photocatalysts. The composition of the samples can be easily tailored by simply varying the $TiCl_4/H_2O$ volume ratio. A proper $TiCl_4/H_2O$ volume ratio is important for the synthesis of a ternary mixture of anatase, brookite, and rutile which exhibits the highest photoactivity.

Note Added after ASAP Publication. This article posted ASAP on July 30, 2009. Sentences 4 and 5 of the 2nd paragraph in the Results section have been revised. The correct version posted on August 6, 2009.

References and Notes

(1) Fujishima, A.; Hashimoto, K.; Watanabe, T. *TiO_2 Photocatalysis: Fundamentals and Applications*; Bkc: Tokyo, 1999.
(2) Bokhimi, X.; Morales, A.; Aguilar, M.; Toledo-Antonio, J. A.; Pedraza, F. *Intern. J. Hydrogen Energy* **2001**, *26*, 1279.
(3) Bickley, R. I.; Gonzales-Carreño, T.; Lees, J. S.; Palmisano, L.; Tilley, R. J. D. *J. Solid State Chem.* **1991**, *92*, 178.
(4) Ohno, T.; Sarukawa, K.; Tokieda, K.; Matsumura, M. *J. Catal.* **2001**, *203*, 82.
(5) Kawahara, T.; Konishi, Y.; Tada, H.; Tohge, N.; Nishii, J.; Ito, S. *Angew. Chem., Int. Ed.* **2002**, *41*, 2811.
(6) Zhang, Q.; Gao, L.; Guo, J. *Appl. Catal. B: Environ.* **2000**, *26*, 207.
(7) Bacsa, R. R.; Kiwi, J. *Appl. Catal. B: Environ.* **1998**, *16*, 19.
(8) Kawahara, T.; Ozawa, T.; Iwasaki, M.; Tada, H.; Ito, S. *J. Colloid Interface Sci.* **2003**, *267*, 377.
(9) Yan, M.; Chen, F.; Zhang, J.; Anpo, M. *J. Phys. Chem. B* **2005**, *109*, 8673.
(10) Li, G.; Gray, K. A. *Chem. Mater.* **2007**, *19*, 1143.
(11) Jiang, D.; Zhang, S.; Zhao, H. *Environ. Sci. Technol.* **2007**, *41*, 303.
(12) Yu, J. C.; Yu, J.; Ho, W.; Zhang, L. *Chem. Commun.* **2001**, 1942.
(13) Yu, J. C.; Zhang, L.; Yu, J. *Chem. Mater.* **2002**, *14*, 4647.
(14) Ozawa, T.; Iwasaki, M.; Tada, H.; Akita, T.; Tanaka, K.; Ito, S. *J. Colloid Interface Sci.* **2005**, *281*, 510.
(15) Cappelletti, G.; Bianchi, C. L.; Ardizzone, S. *Appl. Catal. B: Environ.* **2008**, *78*, 193.
(16) Isley, S. L.; Anderson, E. R.; Penn, R. L. *ECS Trans.* **2006**, *3*, 37.
(17) Ardizzone, S.; Bianchi, C. L.; Cappelletti, G.; Gialanella, S.; Pirola, C.; Ragaini, V. *J. Phys. Chem. C* **2007**, *111*, 13222.
(18) Jiang, K.-J.; Kitamura, T.; Yin, H.; Ito, S.; Yanagida, S. *Chem. Lett.* **2002**, *31*, 872.
(19) Pottier, A.; Chanéac, C.; Tronc, E.; Mazerolles, L.; Jolivet, J.-P. *J. Mater. Chem.* **2001**, *11*, 1116.
(20) Lee, J. H.; Yang, Y. S. *J. Eur. Ceram. Soc.* **2005**, *25*, 3573.
(21) Lee, J. H.; Yang, Y. S. *J. Mater. Sci.* **2005**, *40*, 2843.
(22) Di Paola, A.; Cufalo, G.; Addamo, M.; Bellardita, M.; Campostrini, R.; Ischia, M.; Ceccato, R.; Palmisano, L. *Colloid. Surf. A: Physicochem. Eng. Aspects* **2008**, *317*, 366.
(23) Wei, J.; Yao, J.; Zhang, X.; Zhu, W.; Wang, H.; Rhodes, M. J. *Mater. Lett.* **2007**, *61*, 4610.
(24) Lopez, T.; Gomez, R.; Sanchez, E.; Tzompantzi, F.; Vera, L. *J. Sol-Gel Sci. Technol.* **2001**, *22*, 99.
(25) Wei, F.; Zeng, H.; Cui, P.; Peng, S.; Cheng, T. *Chem. Eng. J.* **2008**, *144*, 119.
(26) Nolph, C. A.; Sievers, D. E.; Kaewgun, S.; Kucera, C J.; McKinney, D. H.; Rientjes, J. P.; White, J. L.; Bhave, R.; Lee, B. I. *Catal. Lett.* **2007**, *117*, 102.
(27) Koelsch, M.; Cassaignon, S.; Guillemoles, J. F.; Jolivet, J.-P. *Thin Solid Films* **2002**, *403−404*, 312.
(28) Zheng, Y.; Shi, E.; Chen, Z.; Li, W.; Hu, X. *J. Mater. Chem.* **2001**, *11*, 1547.
(29) Li, Y.; Fan, Y.; Chen, Y. *J. Mater. Chem.* **2002**, *12*, 1387.
(30) Addamo, M.; Augugliaro, V.; Di Paola, A.; García-López, E.; Loddo, V.; Marcì, G.; Palmisano, L. *Colloid. Surf. A: Physicochem. Eng. Aspects* **2005**, *265*, 23.
(31) Lutterotti, L.; Ceccato, R.; Dal Maschio, R.; Pagani, E. *Mater. Sci. Forum,* **1998**, *278−281*, 87.
(32) Le Bail, A. *J. Non-Cryst. Solids* **1995**, *183*, 39.
(33) Warren, B. E.; Averbach, B. L. *J. Appl. Phys.* **1950**, *21*, 595.
(34) Roy, A. M.; De, G. C.; Sasmal, N.; Bhattacharyya, S. S. *Int. J. Hydrogen Energy* **1995**, *20*, 627.
(35) Wardman, P. *J. Phys. Chem. Ref. Dat.* **1989**, *18*, 1637.
(36) Hünig, S.; Gross, J. *Tetrahedron Lett.* **1968**, *9*, 2599.
(37) Summers, L. A. *Tetrahedron* **1968**, *24*, 5433.
(38) Sing, K. S. W.; Everett, D. H.; Haul, R. A. W.; Moscou, L.; Pierotti, R. A.; Rouquérol, J.; Siemienieniewska, T. *Pure Appl. Chem.* **1985**, *57*, 603.
(39) Koffyberg, F. P.; Dwight, K.; Wold, A. *Solid State Commun.* **1979**, *30*, 433.
(40) Kim, Y. I.; Atherton, S. J.; Brigham, E. S.; Mallouk, T. E. *J. Phys. Chem.* **1993**, *97*, 11802.
(41) Cheng, H.; Ma, J.; Zhao, Z.; Qi, L. *Chem. Mater.* **1995**, *7*, 663.
(42) Jolivet, J.-P. *Metal oxide chemistry and synthesis: from solution to solid state*; Wiley: Chichester, 2000.

(43) Rouquerol, F.; Rouquerol, J.; Singh, K. *Adsorption by powders and porous solids*; Academic Press: San Diego, 1999.
(44) Shibata, T.; Irie, H.; Ohmori, M.; Nakajima, A.; Watanabe, T.; Hashimoto, K. *Phys. Chem. Chem. Phys.* **2004**, *6*, 1359.
(45) Torimoto, T.; Nakamura, N.; Ikeda, S.; Ohtani, B. *Phys. Chem. Chem. Phys.* **2002**, *4*, 5910.
(46) Ward, M.; White, J. R.; Bard, A. J. *J. Am. Chem. Soc.* **1983**, *105*, 27.
(47) Kavan, L.; Grätzel, M.; Gilbert, S. E.; Klemenz, C.; Scheel, H. J. *J. Am. Chem. Soc.* **1996**, *118*, 6716.
(48) Kalyanansundaram, K.; Grätzel, M. *Coord. Chem. Rev.* **1998**, *77*, 347.
(49) Radecka, M.; Rekas, M.; Trenczek-Zajac, A.; Zakrzewska, K. *J. Power Sources* **2008**, *181*, 46.
(50) Grätzel, M.; Rotzinger, F. P. *Chem. Phys. Lett.* **1985**, *118*, 474.
(51) Serpone, N.; Maruthamuthu, P.; Pichat, P.; Pelizzetti, E.; Hidaka, H. *J. Photochem. Photobiol. A: Chem.* **1995**, *85*, 247.
(52) Yan, M.; Chen, F.; Zhang, J.; Anpo, M. *J. Phys. Chem.* **2005**, *109*, 8673.
(53) Ohno, T.; Tokieda, K.; Higashida, S.; Matsumura, M. *Appl. Catal. A: Gen.* **2003**, *244*, 383.
(54) Hurum, D. C.; Agrios, A. G.; Gray, K. A.; Rajh, T.; Thurnauer, M. C. *J. Phys. Chem. B* **2003**, *107*, 4545.
(55) Leytner, S.; Hupp, J. T. *Chem. Phys. Lett.* **2000**, *330*, 231.
(56) Hurum, D. C.; Agrios, A. G.; Crist, S. E.; Gray, K. A.; Rajh, T.; Thurnauer, M. C. *J. Electron Spectrosc. Relat. Phenom.* **2006**, *150*, 155.
(57) Li, Y.; Lee, N.-H.; Song, J. S.; Lee, E. G.; Kim, S.-J. *Res. Chem. Intermed.* **2005**, *31*, 309.
(58) Ovenstone, J. *J. Mater. Sci.* **2001**, *36*, 1325.
(59) Sclafani, A.; Palmisano, L.; Schiavello, M. *J. Phys. Chem.* **1990**, *94*, 829.
(60) Zhang, Q.; Gao, L.; Guo, J. *Appl. Catal. B: Environ.* **2000**, *26*, 207.
(61) García-López, E.; Addamo, M.; Di Paola, A.; Marcì, G.; Palmisano, L. In *Scientific Bases for the Preparation of Heterogeneous Catalysts*; Studies in Surface Science and Catalysis; Gaigneaux, E. M., Devillers, M., De Vos, D. E., Hermans, S., Jacobs, P. A., Martens, J. A., Ruiz, P., Eds.; Elsevier: Amsterdam, 2006; Vol. 162, p 689.
(62) Kim, S.-J.; Lee, E. G.; Park, S. D.; Jeon, C. J.; Cho, Y. H.; Rhee, C. K.; Kim, W. W. *J. Sol-Gel Sci. Technol.* **2001**, *22*, 63.

JP904673E